Molecular Microbiology (2000) **35**(6), 1335–1347

Evidence for donor strand complementation in the biogenesis of *Haemophilus influenzae* haemagglutinating pili

Graham P. Krasan,[1,3] Frederic G. Sauer,[2] David Cutter,[1,3] Monica M. Farley,[4] Janet R. Gilsdorf,[5] Scott J. Hultgren[2] and Joseph W. St. Geme, III[1,2,3]*

[1]Edward Mallinckrodt Department of Pediatrics and [2]Department of Molecular Microbiology, Washington University School of Medicine, and [3]Division of Infectious Diseases, St. Louis Children's Hospital, St. Louis, Missouri, 63110, USA.[4]Veterans Affairs Medical Center and Department of Medicine, Emory University School of Medicine, Decatur, GA, 30033, USA.[5]Department of Pediatrics and Communicable Diseases, University of Michigan Medical School, Ann Arbor, MI, 48109, USA.

Summary

Haemophilus influenzae **haemagglutinating pili are surface appendages that promote attachment to host cells and facilitate respiratory tract colonization, an essential step in the pathogenesis of disease. In contrast to other well-characterized forms of pili, *H. influenzae* haemagglutinating pili are two-stranded helical structures. Nevertheless, haemagglutinating pili are assembled by a pathway that involves a periplasmic chaperone and an outer membrane usher, analogous to the prototype pathway involved in the biogenesis of *Escherichia coli* P pili. In this study, we performed site-directed mutagenesis of the *H. influenzae* HifB chaperone and HifA major pilus subunit at positions homologous to sites important for chaperone–subunit interactions and subunit oligomerization in P pili. Mutations at putative subunit binding pocket residues in HifB or at the penultimate tyrosine in HifA abolished formation of HifB–HifA periplasmic complexes, whereas mutations at the −14 glycine in HifA had no effect on HifB–HifA interactions but abrogated HifA oligomerization. To define further the constraints of the interaction between HifA and HifB, we examined the interchangeability of pilus gene cluster components from *H. influenzae* type b strain Eagan (*hifA-hifE*$_{Eag}$) and the related *H. influenzae* biogroup aegyptius strain F3031 (*hifA-hifE*$_{F3031}$). Functional pili were assembled both with HifA$_{Eag}$ and the strain F3031 gene cluster and with HifA$_{F3031}$ and the strain Eagan gene cluster, underscoring the flexibility of the *H. influenzae* chaperone/usher pathway in incorporating HifA subunits with significant sequence diversity. To gain additional insight into the interactive surfaces of HifA and HifB, we aligned HifA sequences from 20 different strains and then modelled the HifA structure based on the recently crystallized PapD–PapK complex. Analysis of the resulting structure revealed high levels of sequence conservation in regions predicted to interact with HifB, and maximal sequence diversity in regions potentially exposed on the surface of assembled pili. These results suggest broad applicability of structure–function relationships identified in studies of P pili, including the concepts of donor strand complementation and donor strand exchange. In addition, they provide insight into the structure of HifA and suggest a basis for antigenic variation in *H. influenzae* haemagglutinating pili.**

Received 18 October, 1999; revised17 December, 1999; accepted 20 December, 1999. *For correspondence at Department of Molecular Microbiology Washington University School of Medicine, 660 South Euclid, Box 8230, St. Louis, MO 63110, USA. E-mail stgeme@borcim.wustl.edu; Tel. (+1) 314 362 5401; Fax. (+1) 314 362 1232.

Introduction

Haemophilus influenzae is a Gram-negative coccobacillus that is both a commensal organism in the human nasopharynx and an important cause of localized respiratory tract and systemic disease (Turk, 1984). Diverse isolates of *H. influenzae* express a variety of pilus and non-pilus adhesive factors (Rao *et al*., 1999) involved in recognition of specific eukaryotic receptor motifs (Karlsson, 1989; Hultgren *et al*., 1996). Perhaps best-characterized among *H. influenzae* adhesins are haemagglutinating pili, which are expressed by encapsulated and a subset of non-encapsulated (non-typable) strains (Stull *et al*., 1984; Gilsdorf *et al*., 1992; Krasan *et al*., 1999). These structures agglutinate AnWj-positive erythrocytes and mediate attachment to human oropharyngeal cells and respiratory tissue in organ culture (van Alphen *et al*., 1986; Loeb *et al*., 1988; Farley *et al*., 1990; Read *et al*., 1991). In addition, they facilitate nasopharyngeal colonization in monkeys (Weber *et al*., 1991).

Based on examination by quick-freeze, deep-etch transmission electron microscopy, *H. influenzae* haemagglutinating pili are known to be composite polymeric

structures, consisting of a two-stranded helical rod capped by a short tip fibrillum (St. Geme *et al*., 1996). The *H. influenzae* pilus gene cluster has been cloned and sequenced from type b and non-typable strains and consists of five genes, designated *hifA–hifE* (van Ham *et al*. 1994; McCrea *et al*., 1994; 1997; Watson *et al*., 1994; Geluk *et al*., 1998; Mhlanga-Mutangadura, 1998). The *hif* gene products share homology with proteins involved in the biogenesis of other pili, including P pili produced by uropathogenic *Escherichia coli* (Hultgren *et al*., 1996).

hifA encodes the major structural subunit (HifA) of *H. influenzae* haemagglutinating pili and is transcribed divergently from the remainder of the gene cluster (van Ham *et al*., 1994). Upstream of *hifA*, the *hifB* gene encodes a chaperone (HifB), the *hifC* gene encodes a putative outer membrane usher (HifC) and the *hifD* and *hifE* genes encode minor structural subunits (HifD and HifE) (van Ham *et al*., 1994; McCrea *et al*., 1994; 1997; Watson *et al*., 1994; St. Geme *et al*., 1996). Existing evidence indicates that *H. influenzae* haemaglutinating pili are assembled by the chaperone/usher pathway, originally defined in P-piliated *E. coli* (Thanassi *et al*., 1998). HifB forms periplasmic complexes with HifA, HifD and HifE, and stabilizes these subunits, then presumably delivers them to HifC for translocation across the outer membrane (St. Geme *et al*., 1996). Ultimately HifA is incorporated throughout the pilus shaft, whereas HifD and HifE make up the tip fibrillum (St. Geme *et al*., 1996; McCrea *et al*., 1997). Preliminary evidence suggests that HifE is the adhesive subunit (McCrea *et al*., 1997).

PapD is the periplasmic chaperone involved in the assembly of P pili and is the prototype member of a large family of bacterial chaperones involved in interactions with pilin subunits (Holmgren *et al*., 1992; Hultgren *et al*., 1996; Hung *et al*., 1996). The crystal structures of PapD alone (Holmgren *et al*., 1992) and PapD interacting with the PapK pilin subunit (Sauer *et al*., 1999) have been solved. PapD consists of two immunoglobulin-like (Ig) folds oriented in an L-shape with an intervening cleft. The PapK subunit consists of a single Ig fold but lacks the expected seventh, C-terminal β strand (strand G). The absence of this strand leaves a deep groove along the surface of PapK and exposes its hydrophobic core, predisposing the subunit to aggregation and degradation. In the PapD–PapK complex, the G1 strand of PapD occupies the groove in PapK and completes the Ig fold, a phenomenon referred to as donor strand complementation (Choudhury *et al*., 1999; Sauer *et al*., 1999). This interaction shields the hydrophobic core of the subunit and thus stabilizes the protein. Within the groove, the G1 strand of PapD interacts on one side with the C-terminal, F strand of PapK. The Arg-8 and Lys-112 residues in the PapD cleft serve to anchor the C-terminal end of the F strand (Slonim *et al*., 1992; Kuehn *et al*., 1993; Hung *et al*., 1996). Mutational and biochemical studies indicate that residues in the F strand of PapK and other Pap subunits also participate in primary 'head-to-tail' and secondary packaging interactions between subunits in assembled pili (Bullitt *et al*., 1996; Soto *et al*., 1998). The glycine located 14 residues from the C-terminal end of subunits (−14 position) is especially important for these interactions (Bullitt *et al*., 1996; Soto *et al*., 1998).

Given the unusual two-stranded architecture of *H. influenzae* haemagglutinating pili, in the present study we performed site-directed mutagenesis of HifB and HifA to investigate the structural motifs predicted to comprise chaperone–subunit and subunit–subunit interfaces. In addition, we examined the constraints on the HifB–HifA interaction by assessing the interchangeability of pilus gene cluster components from two diverse *H. influenzae* strains. Finally, we combined information from the crystal structure of the PapD–PapK complex and from HifA sequences from 20 different strains to model the structure of HifA and gain further insight into the interactive surfaces of HifB and HifA.

Results

HifB and HifA contain components of a chaperone–subunit molecular anchor motif

In the P pilus system, the Arg-8 and Lys-112 residues in the PapD cleft anchor the C-terminal end of the F strand of a given subunit and position the G1 strand of PapD relative to the F strand to complete the Ig fold of the subunit. Mutations at either Arg-8 or Lys-112 abolish chaperone–subunit complex formation, indicating the critical role of these residues in donor strand complementation (Slonim *et al*., 1992; Kuehn *et al*., 1993). To determine whether the HifB chaperone has a similar molecular anchor, we focused on *H. influenzae* strain Eagan and mutated the homologous residues in the strain Eagan HifB protein

Fig. 1. A. Sequence alignment of PapD with HifB from *H. influenzae* strain Eagan and from *H. influenzae* biogroup agyptius strain F3031. Residues conserved throughout the PapD chaperone superfamily are highlighted by boxes. Invariant residues changed by site-directed mutagenesis are indicated by arrows. Residues that differ between the *H. influenzae* strain Eagan and the *H. influenzae* biogroup agyptius strain F3031 HifB proteins are indicated by an asterisk. Alignment data are adapted from Hung *et al.* (1996) and Soto *et al.* (1998). PapD is 45% similar to the strain Eagan HifB protein and 44% similar to the strain F3031 HifB protein.
B. Sequence alignment of HifA from *H. influenzae* strain Eagan and from *H. influenzae* biogroup agyptius strain F3031. Identical residues are indicated by an asterisk (*). Residues homologous to those comprising conserved N-terminal and C-terminal regions in other pilus subunits in the chaperone/usher superfamily are highlighted by boxes. Residues changed by site-directed mutagenesis are denoted by arrows. The underlined sequence represents the signal sequence.

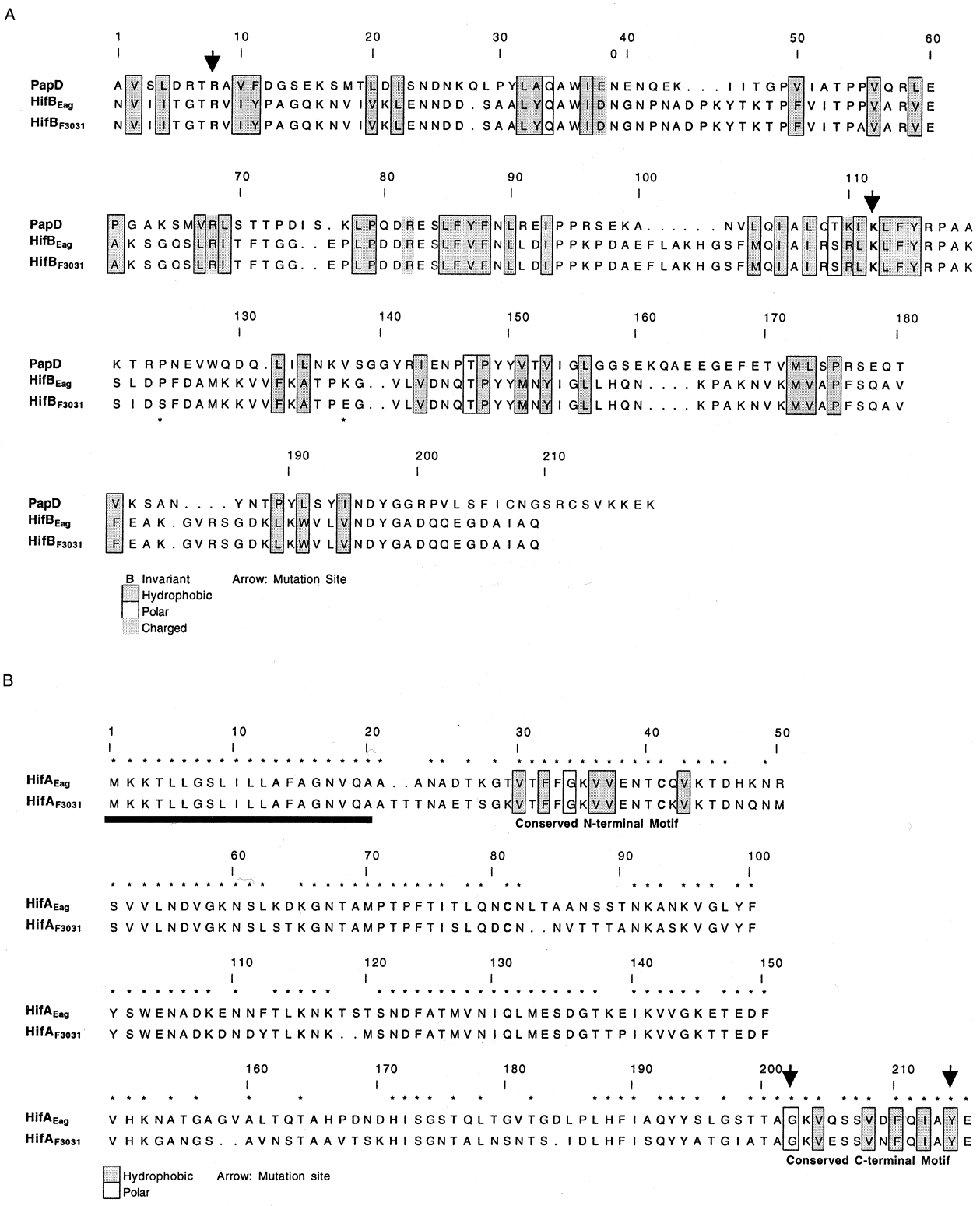

(Arg-9 and Lys-119 respectively), replacing the Arg-9 residue with a glycine and the Lys-119 residue with an alanine (Fig. 1A). These substitutions strip the basic side chains from the original amino acids and are not predicted to cause major perturbations in protein conformation. The resulting *hifB* mutants were then co-expressed with pJS201 ($hifA_{Eag}$) in *E. coli* ORN103. In control experiments, we confirmed that the HifB derivatives were localized properly to the periplasm (not shown). As shown in Fig. 2A, when either pJS202.1 [$HifB_{Eag}$(R9G)] or pJS202.2 [$HifB_{Eag}$(K119A)] was co-expressed with pJS201, we were unable to detect HifA in the periplasm, consistent with periplasmic degradation.

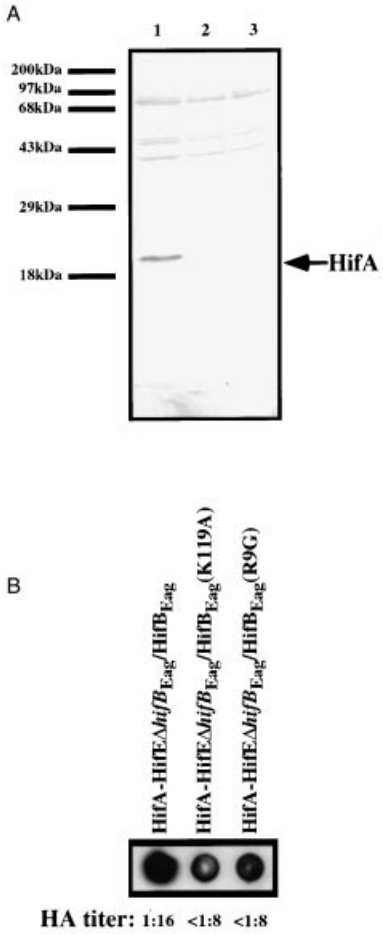

Fig. 2. A. Western analysis of periplasmic proteins from *E. coli* ORN103, containing pJS201 (*hifA*) complemented with either wild-type *hifB* (pJS202) or the mutant derivatives $HifB_{Eag}$(K119A) (pJS202.1) and $HifB_{Eag}$(R9G) (pJS202.2), probed with anti-HifA antiserum. Samples were loaded as follows: lane 1, ORN103/pJS201+pJS202; lane 2, ORN103/pJS201+pJS202.1; lane 3, ORN103/pJS201+pJS202.2. The monomeric HifA species is indicated by an arrow.
B. Dot immunoblots of *E. coli* ORN103, carrying pWW15Δ*hifB* (*hifA-hifE*$_{Eag}$ with an in frame deletion in *hifB*) complemented with either wild-type *hifB* (pJS202) or the mutant derivatives $HifB_{Eag}$(K119A) (pJS202.1) or $HifB_{Eag}$(R9G) (pJS202.2), probed with anti-HifB-HifA antiserum. Semi-quantitative haemagglutination (HA) titres from the same ORN103 derivatives are indicated below the respective dot immunoblot samples.

To assess the ramifications of these binding pocket mutations on pilus biogenesis, the *hifB* mutants were co-expressed with pWW15Δ*hifB*, which contains the entire pilus gene cluster from strain Eagan with an in frame deletion in *hifB*. Examination of periplasmic proteins revealed abundant HifA in ORN103/pWW15, but no detectable HifA in ORN103/pWW15Δ*hifB* (not shown). As expected, complementation of pWW15Δ*hifB* with wild-type $hifB_{Eag}$ resulted in rescue of HifA in the periplasm and production of surface-localized pili, as measured by haemagglutination assays and whole cell dot immunoblots (Fig. 2B). In contrast, ORN103 derivatives harbouring pWW15Δ*hifB* together with either pJS202.1 [$HifB_{Eag}$(R9G)] or pJS202.2 [$HifB_{Eag}$(K119A)] were haemagglutination-negative and failed to react significantly with anti-HifB/HifA antiserum in whole cell dot immunoblots (Fig. 2B). The failure to produce mature pili when non-conservative residues were substituted at Arg-9 and Lys-119 underscores the importance of these positions as a molecular anchor in chaperone–subunit complex formation and pilus biogenesis.

To complement analysis of the HifB subunit binding pocket, we determined whether the C-terminal, F strand of HifA functions in donor strand complementation. An important feature of the F strand in P-pilus subunits is the penultimate aromatic residue, which interacts with the G1 strand of the chaperone. Accordingly, we targeted the tyrosine at position 215 in the strain Eagan HifA protein and examined whether mutation of this residue disrupts possible primary interactions with the chaperone (Fig. 1B). Our approach involved the generation of three separate point mutations at this site, including a conservative change that preserves the aromatic side-chain [$HifA_{Eag}$(Y215F)], a non-conservative substitution [$HifA_{Eag}$(Y215S)] and a deletion of both the penultimate and terminal residues [$HifA_{Eag}$(Y215Stop)]. The resulting constructs were co-expressed with pJS202 ($HifB_{Eag}$), and periplasmic extracts were examined by immunoblot assay with anti-HifA antiserum. As shown in Fig. 3A, mutation of Tyr-215 to phenylalanine had little effect on the quantity of HifA in the periplasm. In contrast, with $HifA_{Eag}$(Y215S) and $HifA_{Eag}$(Y215Stop), HifA was undetectable, suggesting an unstable HifB–HifA interaction.

To assess the influence of the HifA Tyr-215 residue on pilus biogenesis, the *hifA* mutants were co-expressed with pWW1, which contains *hifB-hifE*$_{Eag}$. In control experiments, co-expression of wild-type $hifA_{Eag}$ (pJS201) with pWW1 resulted in the production of functional surface-associated pili, as measured by haemagglutination assays, whole cell dot immunoblot assays and negative straining transmission electron microscopy (Fig. 3B and not shown). Consistent with our analysis of HifA levels in periplasmic extracts, co-expression of pJS206.1 [$HifA_{Eag}$(Y215F)] and

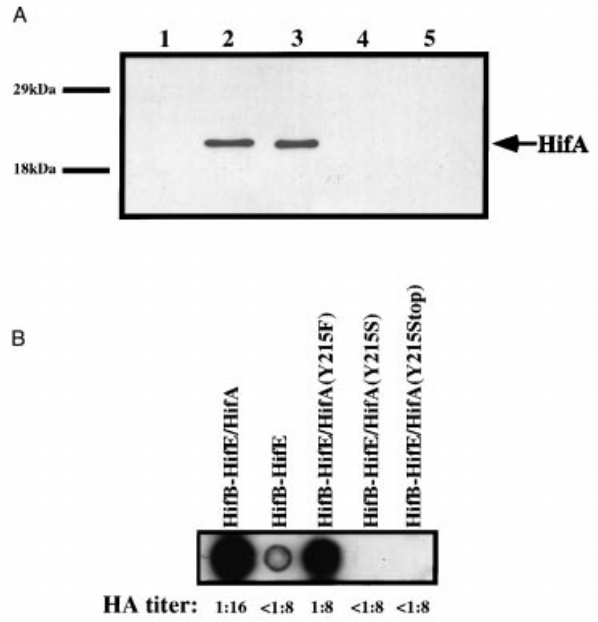

Fig. 3. A. Western analysis of periplasmic proteins from *E. coli* ORN103 carrying *hifB*$_{Eag}$ (pJS202) complemented with either wild-type *hifA*$_{Eag}$ (pJS201) or the mutant derivatives HifA$_{Eag}$(Y215F) (pJS201.1), HifA$_{Eag}$(Y215S) (pJS201.2) and HifA$_{Eag}$(Y215Stop) (pJS201.3), probed with anti-HifA antiserum. Samples were loaded as follows: lane 1, ORN103/pJS202; lane 2, ORN103/pJS201+pJS202; lane 3, ORN103/pJS201.1+pJS202; lane 4, ORN103/pJS201.2+pJS202; lane 5, ORN103/pJS201.3+pJS202. The mature HifA species is indicated by an arrow.
B. Dot immunoblots of *E. coli* ORN103 with pWW1 (*hifB-hifE*$_{Eag}$) alone or complemented with either wild-type *hifA* (pJS206) or the mutant derivatives HifA$_{Eag}$(Y215F) (pJS201.1), HifA$_{Eag}$(Y215S) (pJS201.2) and HifA$_{Eag}$(Y215Stop) (pJS201.3), probed with anti-HifB-HifA antiserum. Semi-quantitative haemagglutination (HA) titres from the same ORN103 derivatives are indicated below the respective dot immunoblot samples.

pWW1 was associated with appreciable haemagglutination and significant reactivity in whole cell dot immunoblots, whereas analysis of either pJS206.2 [HifA$_{Eag}$(Y215S)] or pJS206.3 [HifA$_{Eag}$(Y215Stop)] with pWW1 revealed absent haemagglutination and negligible reactivity with anti-HifB-HifA antiserum. These results highlight the critical nature of the penultimate tyrosine, especially when the aromatic side chain is removed.

Glycine-203 of HifA is critical for subunit–subunit interactions

In additional experiments, we found that polymerization of strain Eagan HifA subunits could be appreciated by comparing boiled and unboiled samples of periplasmic HifB–HifA complexes resolved on SDS–PAGE gels. Whereas boiling was associated with only monomeric HifA, omission of boiling resulted in a striking ladder of bands corresponding to dimers, trimers and higher order HifA multimers (Fig. 4A, compare lanes 3 boiled and unboiled). This finding complements our previous observation that purified HifB–HifA complexes serve as building blocks for spontaneous assembly of HifA subunits into pilus-like structures (St. Geme *et al.*, 1996).

In the case of P pili, subunit–subunit interactions involve F strand residues, including the glycine at position −14 from the C-terminus (Bullitt *et al.*, 1996; Soto *et al.*, 1998). With this information in mind, we mutated the corresponding identical residue in the strain Eagan HifA protein (Gly-203), converting this amino acid to either

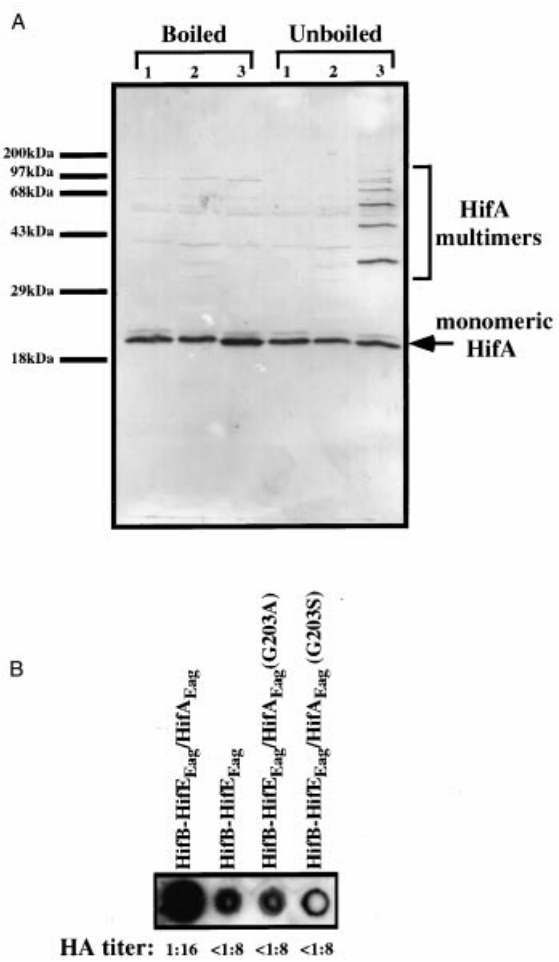

Fig. 4. A. Western analysis of boiled and unboiled periplasmic proteins from *E. coli* ORN103 carrying *hifB*$_{Eag}$ (pJS202) complemented with either wild-type *hifA*$_{Eag}$ (pJS201) or the C-terminal −14 glycine mutant derivatives HifA$_{Eag}$(G203A) (pJS201.4) and HifA$_{Eag}$(G203S) (pJS201.5), probed with anti-HifA antiserum. Samples were loaded as follows: lane 1, ORN103/pJS201.4+pJS202; lane 2, ORN103/pJS201.5+pJS202; lane 3, ORN103/pJS201+pJS202. The monomeric HifA species is indicated by an arrow and HifA multimers are indicated by a bracket.
B. Dot immunoblots of *E. coli* ORN103 with pWW1 (*hifB-hifE*$_{Eag}$) alone or complemented with either wild-type *hifA* $_{Eag}$ (pJS206) or the mutant derivatives HifA$_{Eag}$(G203A) (pJS201.4) and HifA$_{Eag}$(G203S) (pJS201.5), probed with anti-HifB-HifA antiserum. Haemagglutination (HA) titres from the same ORN103 derivatives are indicated below the respective dot immunoblot samples.

alanine or serine. As shown in Fig. 4A, comparison of periplasmic extracts from ORN103 producing HifB and either wild-type $HifA_{Eag}$, $HifA_{Eag}$(G203 A) or $HifA_{Eag}$(G203S) revealed no appreciable difference in the quantity of monomeric HifA present after boiling, electrophoresis and immunoblot analysis. However, mutation of Gly-203 abolished the ability to form multimers (Fig. 4A), supporting the conclusion that this residue is important in HifA–HifA interactions without affecting HifB–HifA interactions and HifA stability.

To extend these observations, we co-expressed the *hifA* Gly-203 mutants with pWW1 and then performed haemagglutination assays, whole cell dot immunoblot assays and transmission electron microscopy. As predicted from our analysis of multimer formation, $HifA_{Eag}$(G203A) and $HifA_{Eag}$(G203S) were not incorporated into mature pili (Fig. 4B). These results underscore the importance of the −14 glycine in assembly of *H. influenzae* pili.

The HifA subunit can be incorporated into functional pili by the heterologous pilus gene cluster from H. influenzae *biogroup aegyptius strain F3031 and vice versa*

To begin to identify other residues important in chaperone–subunit interactions or assembly of mature *H. influenzae* pili, we performed cross-complementation analysis of the pilus gene cluster from strain Eagan with the pilus assembly system in *H. influenzae* biogroup aegyptius strain F3031 (the hif_{F3031} gene cluster). Initially, we examined whether non-conservative sequence differences between $HifA_{Eag}$ and $HifA_{F3031}$ (Fig. 1B) would affect interaction with HifB. In particular, we co-expressed either $hifA_{Eag}$ (pJS206) and *hifB-*$hifE_{F3031}$ (pGK203) or $hifA_{F3031}$ (pGK201) and *hifB-*$hifE_{Eag}$ (pWW1) and then extracted periplasmic proteins and performed immunoblot analysis with anti-HifA antiserum. As shown in Fig. 5A, appreciable quantities of $HifA_{Eag}$ and $HifA_{F3031}$ were detected with both the homologous and the heterologous assembly proteins.

In additional experiments we examined the same strains and assessed formation of functional pili. In whole cell dot immunoblots, reactivity with anti-HifB-HifA antiserum was similar with $HifA_{Eag}$ plus HifB-$HifE_{Eag}$, $HifA_{Eag}$ plus HifB-$HifE_{F3031}$, $HifA_{F3031}$ plus HifB-$HifE_{F3031}$, and $HifA_{F3031}$ plus HifB-$HifE_{Eag}$ (Fig. 5B). Interestingly, this measure of pilus density did not correlate with the relative haemagglutination titres. Instead, both ORN103 derivatives with HifB-$HifE_{Eag}$ were associated with haemagglutination titres of 1:16, whereas both strains with HifB-$HifE_{F3031}$ were associated with titres of 1:128 (Fig. 5B). To explore the reason for these results, all four strains were examined using negative staining transmission electron microscopy. Despite moderate cell-to-cell variation in pilus density, no differences overall were apparent among these strains in either density or morphology of pili (Fig. 6). One possibility is that the $HifE_{Eag}$ and $HifE_{F3031}$ subunits, the putative adhesins, have differing affinities for the same erythrocyte receptor. Alternatively, it is possible that different amounts of $HifE_{Eag}$ versus $HifE_{F3031}$ are presented on the bacterial surface.

Finally, we examined the role of residues that distinguish $HifB_{Eag}$ from $HifB_{F3031}$ (Fig. 1A) by co-expressing pWW15Δ*hifB* and $hifB_{F3031}$ and then assessing pilus assembly. Interestingly, ORN103, harbouring both pWW15Δ*hifB* and pJS205 ($hifB_{F3031}$), was associated with haemagglutination titres and reactivity on dot immunoblots similar to those observed with co-expression of pWW15Δ*hifB* and the homologous chaperone (not shown).

Modelling of the HifA structure reveals marked sequence conservation in regions predicted to interact with HifB

To gain additional insight into the interactive surfaces of HifA and HifB, we began by aligning available HifA amino

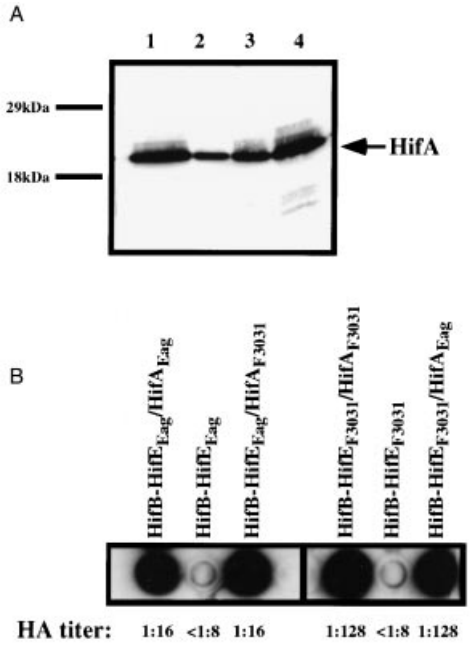

Fig. 5. A. Western analysis of periplasmic proteins from *E. coli* ORN103 containing either pWW1 (*hifB-*$hifE_{Eag}$) or pGK203 (*hifB-*$hifE_{F3031}$), complemented with either wild-type $hifA_{Eag}$ (pJS206) or wild-type $hifA_{F3031}$ (pGK201), probed with anti-HifA antiserum. Samples were loaded as follows: lane 1, ORN103/pWW1+pJS206; lane 2, ORN103/pWW1+pGK201; lane 3, ORN103/pGK203+pGK201; lane 4, ORN103/pGK203+pJS206. The mature HifA species is indicated by an arrow.
B. Dot immunoblots of *E. coli* ORN103 with either pWW1 (*hifB-*$hifE_{Eag}$) or pGK203 (*hifB-*$hifE_{F3031}$) alone, or complemented with either wild-type $hifA_{Eag}$ (pJS206) or $hifA_{F3031}$ (pGK201), probed with anti-HifB-HifA antiserum. Haemagglutination (HA) titres from the same ORN103 derivatives are indicated below the respective dot immunoblot samples.

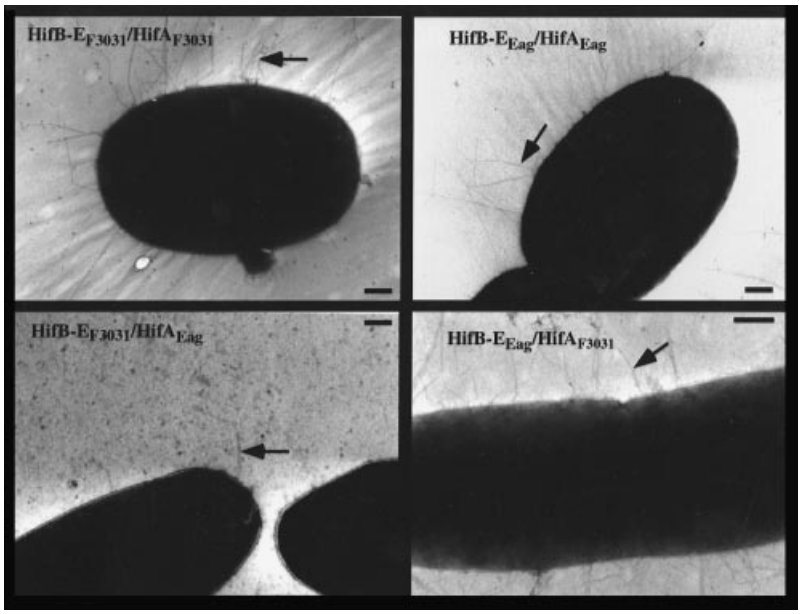

Fig. 6. Negative-stained electron micrographs of *E. coli* ORN103 containing either the F3031 gene cluster (pGK203) complemented with wild-type *hifA*$_{F3031}$ (upper left panel), the F3031 gene cluster (pGK203) complemented with wild-type *hifA*$_{Eag}$ (lower left panel), the Eagan gene cluster (pWW1) complemented with wild-type *hifA*$_{Eag}$ (upper right panel) or the Eagan gene cluster (pWW1) complemented with wild-type *hifA*$_{F3031}$ (lower right panel). In each panel, pili are indicated by arrows. The bars represent 100 nm.

acid sequences from 20 different *H. influenzae* strains and then comparing these sequences with the amino acid sequence of the PapK subunit that was crystallized together with PapD (Sauer *et al*., 1999). As shown in Fig. 7A, using the strain Eagan HifA protein as a reference, alignment of the HifA sequences revealed striking homology between residues 1–61, 73–96, 103–132 and 167–197. As a corollary, maximal sequence diversity was concentrated in the three regions delimited by residues 62–72, 97–102 and 104–166. Interestingly, comparison of the HifA sequences and the PapK structure strongly suggests that HifA is a C-terminally truncated Ig fold. The two cysteines involved in disulphide bond formation, the hydrophobic core residues and all of the residues that participate in donor strand complementation in PapK are conserved between all of the HifA sequences and PapK.

Given the conservation of structural features between HifA and PapK, we chose to model the HifA structure based on the PapK crystal structure. Our goal was to address the level of amino acid sequence and structural conservation among HifA proteins in regions predicted to interact with the HifB chaperone. Figure 7B shows the hypothetical HifA structure. Yellow indicates structural residues that are conserved between HifA and PapK, whereas blue-purple indicates residues that are conserved among HifA sequences (with identity in at least 16 of the 20 sequences). The maximally divergent regions of HifA, including residues 62–72, 97–102 and 104–166, are coloured red and are shown as loops projecting away from the rest of the molecule. Of note, these regions represent insertions relative to the PapK sequence, thus precluding accurate modelling of their conformation.

Examination of the hypothetical HifA structure together with a chaperone reveals high level sequence and structural conservation in all areas potentially interacting with the chaperone. In contrast, the hypervariable regions are confined to three separate sites that are unlikely to interact with the chaperone. These regions are exposed on the surface of the molecule and are potentially exposed in assembled pili. Of note, previous investigators identified three relatively hydrophilic regions within HifA sequences and originally proposed that these regions might constitute highly conserved antigenic epitopes (Forney *et al*., 1991). However, in subsequent studies, antisera raised against peptides corresponding to these regions failed to react with native pili (Gilsdorf *et al*., 1993). Based on the hypothetical HifA structure, these three regions (corresponding to amino acids 15–33, 79–95 and 122–132 in the mature Eagan HifA protein) contribute to the A, C and D β-sheets and are likely to be obscured in mature pili. In additional work, Palmer and Munson described a monoclonal antibody designated 3H12 that appeared to react specifically with an epitope present in strain M37 pili and absent from strain MinnA pili (1992). Mapping of this strain-specific epitope localized it to a region that includes the two hypervariable regions between amino acids 62–72 and 97–102 (Palmer and Munson, 1992), providing strong evidence that these regions are surface-exposed in native pili.

Discussion

H. influenzae haemagglutinating pili possess a number of characteristics reminiscent of P pili. In particular, they are composite fibres consisting of a thick rod joined to a thin tip fibrillum; their assembly involves a periplasmic chaperone

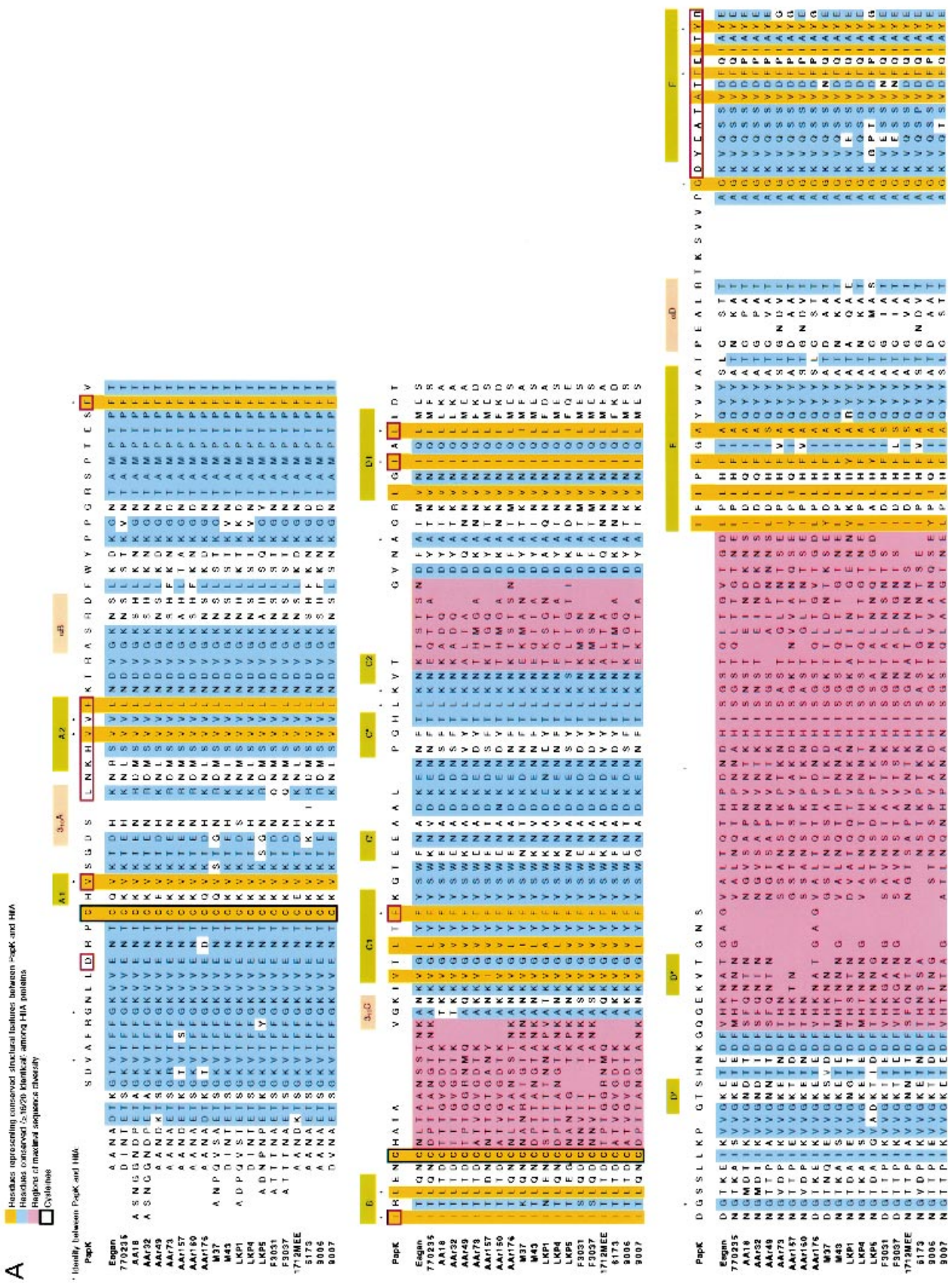
A
Identity between PapK and HIA
Hasidaes representing conserved structural features between PapK and HIA
Hasidaes conserved (≥18/20 identical) among HIA proteins
Regions of maximal sequence diversity
Cysteine
PapK
Egan
770235
AA18
AAr32
AAr49
AAr73
AAr157
AAr150
AAr176
M37
M43
LKP1
LKP4
LKP5
F3031
F3037
1712MEE
8173
9006
9007

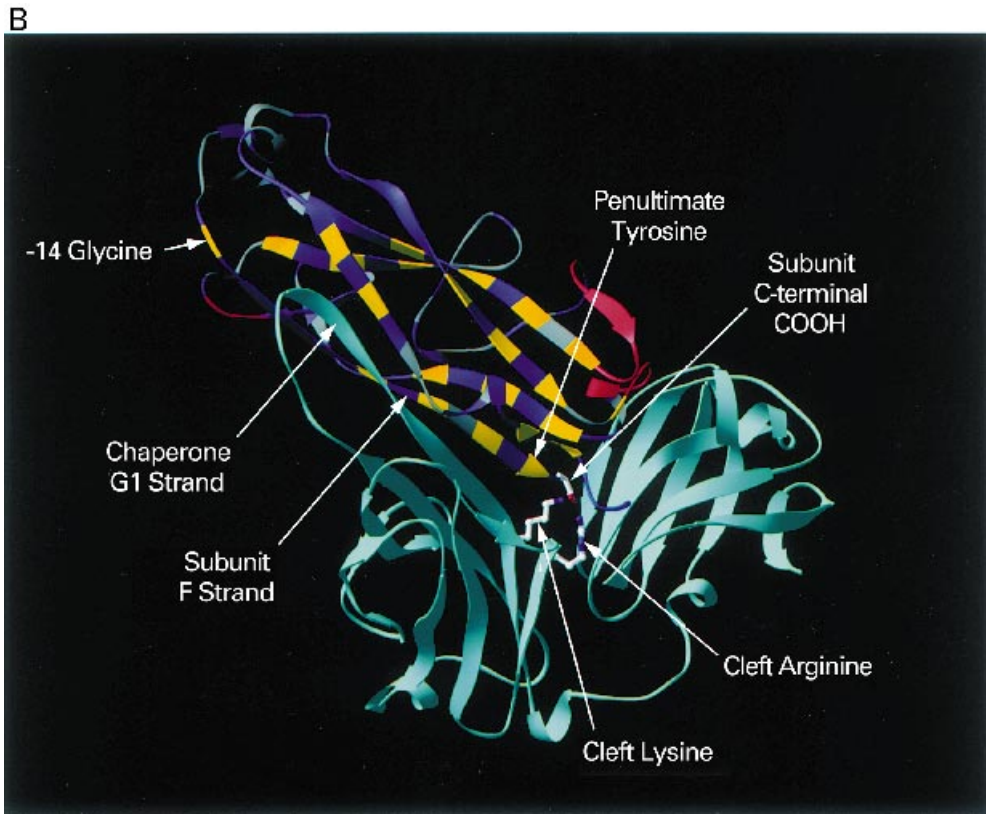

Fig. 7. A. Alignment of PapK and predicted amino acid sequences of HifA from 20 different *H. influenzae* strains. The secondary structural elements of PapK are indicated above the aligned sequences with β-strands in light green boxes and α-or 3-helices in peach boxes. PapK residues involved in contact with domain 1 of PapD are boxed in red. Asterisks denote residues that are identical between PapK and all HifA sequences. Residues highlighted in yellow correspond to conserved structural features between PapK and HifA. Residues highlighted in blue are conserved among HifA proteins (identity in at least 16 of the sequences). Sequences shaded pink represent maximally divergent regions in HifA. PapK is 33% similar to the strain Eagan HifA protein.
B. A ribbon diagram (program RIBBONS; Carson, 1997) of HifA based on the structure of PapK in the PapD–PapK complex. PapD is in cyan. Residues in HifA are colour coded according to the sequence alignment in panel A. Yellow indicates amino acids that are conserved between the 20 HifA sequences and PapK and correspond to residues critical to the structure of PapK, including the two cysteines that form a disulphide bond, all of the residues that participate in donor strand complementation in PapK and nearly all of the hydrophobic core residues. Blue-purple indicates amino acids that are strictly conserved among the 20 HifA sequences. Red indicates regions that are maximally divergent in HifA. These regions represent insertions relative to PapK (see Fig. 7A) and were not modelled. The chaperone G1 strand (which completes the Ig fold of the subunit) and the subunit F strand, including the penultimate tyrosine and the −14 glycine residues, are indicated. The −14 glycine is located 14 residues from the C-terminal end of the subunit. The side chains of the arginine and lysine residues in the chaperone cleft (Arg-8 and Lys-112 in PapD, corresponding to Arg-9 and Lys-119 in HifB) are shown making salt bridge interactions on either side of the C-terminal carboxylate of the subunit. Atoms in these side chains are colour coded white for carbon, red for oxygen and blue for nitrogen.

(HifB) and an outer membrane usher (HifC); and purified complexes containing HifB and the major structural subunit (HifA) spawn the spontaneous self-assembly of HifA into rod-like structures (St. Geme *et al.* 1996; Gilsdorf *et al.*, 1997). On the other hand, two significant departures from the P pilus system include a two-stranded architecture and a greater economy of genes necessary for pilus assembly (5 rather than 11) (van Ham *et al.*, 1994; St. Geme *et al.*, 1996). Whether the molecular basis of chaperone–subunit and subunit–subunit interactions might be different has been unclear.

More than 30 PapD-like periplasmic chaperones have been identified, including the HifB chaperone involved in the assembly of *H. influenzae* haemagglutinating pili. In the present study, we targeted the HifB Arg-9 and Lys-119 residues, which are invariant among members of the PapD superfamily and, in the case of PapD, participate in donor strand complementation (Hung *et al.*, 1996; Sauer *et al.*, 1999). Of note, mutation of these residues abolished HifB–HifA interactions and eliminated formation of pili. In P pilus subunits, the penultimate tyrosine residue interacts with the G1 strand of PapD and is critical for pilus assembly. Comparison of HifA sequences from 20 different strains reveals a penultimate tyrosine in all cases. Interestingly, when this amino acid was replaced by another aromatic residue in the Eagan HifA protein, productive interaction between HifA and HifB was still possible and pilus assembly proceeded, although with

slightly reduced efficiency. In contrast, substitution with serine abolished pilus formation. Thus, substitutions at canonical positions in either the chaperone or the subunit disrupt HifB–HifA complexes, arguing that HifB stabilizes subunits via a donor strand complemenation mechanism.

Subunits assembled by the chaperone/usher pathway possess an N-terminal extension (residues 1–13 in PapK) with a highly conserved motif that has been shown to participate in subunit–subunit interactions (Soto *et al*., 1998). This motif consists of alternating hydrophobic amino acids and is similar to the PapD G1 strand involved in donor strand complementation. Based on the crystal structure of PapK, the N-terminal extension does not contribute to the Ig fold, instead projecting away from the fold and free to interact with another subunit (Sauer *et al*., 1999). With this information in mind, during pilus biogenesis, the N-terminal extension of one subunit is believed to displace the chaperone G1 strand from the neighbouring subunit in a process termed donor strand exchange (Choudhury *et al*., 1999; Sauer *et al*., 1999). Accordingly, the mature pilus should consist of an array of perfectly canonical Ig folds, each containing a strand from the preceding subunit. In this context, it is noteworthy that mutation of the PapA −14 residue from gycine to alanine changed the helical symmetry of pili, and mutation from glycine to tyrosine reduced assembly of pili (Bullitt *et al*., 1996). Similarly, mutation of the HifA −14 glycine to either alanine or serine completely disrupted HifA polymerization, suggesting that assembly of *H. influenzae* haemagglutinating pili may also occur via donor strand exchange.

Comparison of HifA amino acid sequences from multiple strains demonstrates significant diversity. Despite this diversity, in cross-complementation studies, we found that the HifB chaperone from strain Eagan was capable of interacting with both the strain Eagan HifA and the strain F3031 HifA. Similarly, the HifB chaperone from strain F3031 demonstrated productive interaction with both the strain F3031 and the strain Eagan HifA molecules. Considered together, these observations suggest that residues involved in donor strand complementation and donor strand exchange are conserved among different Hif subunits and HifB chaperones. Consistent with this possibility, in the modelled HifA structure, regions predicted to interact with HifB are highly conserved. As a corollary, the three hypervariable regions in HifA correspond to presumed loops between β strands and are unlikely to be involved in either HifB–HifA or HifA–HifA interactions.

Native *H. influenzae* pili demonstrate a high degree of immunologic heterogeneity with both polyclonal antisera and monoclonal antibodies (Brinton *et al*., 1989; Gilsdorf *et al*., 1990; 1992; Palmer and Munson, 1992). Based on studies by Brinton and co-workers using antisera against whole pili, haemagglutinating pili can be separated into at least 14 different serological groups (1989). In recent work, Clemens *et al*. (1998) proposed that the non-conserved sequences present across HifA lineages might be a basis for pilus antigenic variation. Examination of the modelled HifA structure supports this hypothesis, as hypervariable regions reside on the surface of the HifA molecule, away from sequences that form the groove and are likely to participate in subunit–subunit interactions. Experimental results with monoclonal antibody 3H12 argue that at least two of the three hypervariable regions are exposed on native pili. In particular, this antibody reacts specifically with an epitope present in native pili from *H. influenzae* strain M37 but not other strains, and mapping of this epitope has localized it to a region that includes the two hypervariable regions between amino acids 62–72 and 97–102 (Palmer and Munson, 1992).

There are several potential limitations to sudying *H. influenzae* pilus expression in *E. coli* rather than the parental background. Considerations include the decoupling of bidirectional transcription by co-expressing *hifA* and *hifB* on different plasmids, over-expression of the major structural subunit ($HifA_{Eag}$ or $HifA_{F3031}$), resulting in saturation of chaperones and usher sites and interference with the efficient export of HifD or HifE, and the loss of possible regulatory units and feedback mechanisms that may modulate pilus assembly. In light of these limitations, we restricted our goals in this study to dissecting the structural details of pilus biogenesis by site-directed mutagenesis and reconstitution of pilus assembly. Further details related to pilus assembly and function may necessitate reconstitution in the original *H. influenzae* background.

To summarize, our results emphasize the broad applicability of the paradigm for pilus biogenesis identified in studies of P pili, including the concepts of donor strand complementation and donor strand exchange. In addition, they provide new information about the structure of the HifA subunit and suggest a structural explanation for antigenic variation in *H. influenzae* haemagglutinating pili.

Experimental procedures

Bacterial strains and plasmids

H. influenzae strain Eagan is a type b strain that contains the intact *hif* gene cluster (hif_{Eag}) (McCrea *et al*., 1994). *H. influenzae* biogroup aegyptius strain F3031 contains the hif_{F3031} gene cluster, which is homologous to the hif_{Eag} gene cluster (Read *et al*., 1996). *E. coli* DH5α was used for cloning purposes (Sambrook *et al*., 1989) and ORN103 served as the host strain for all complementation studies (Orndorf and Falkow, 1984). The plasmid constructs used in this study are described in Table 1. Plasmids pJS201 and pJS206 contain the $hifA_{Eag}$ gene as an *Eco*RI–*Bam*HI fragment and are identical except for the vector backbone and the corresponding inducible promoter. Similarly, pJS202 and pJS204 contain the $hifB_{Eag}$ gene as an *Eco*RI–*Bam*HI fragment and

Table 1. Plasmid constructs.

Plasmid	Description	Reference
pGEM5	Amp^R	Promega
pMMB91	Kan^R	Furste *et al*. (1986)
pOK12	Kan^R	Viera and Messing (1991)
pTrc99 A	Amp^R	Amann *et al*. (1988)
pUC19	Amp^R	Yanisch-Perron *et al*. (1985)
pAW513	pUC19-*hifA*$_{F3031}$	Whitney and Farley (1993)
pJS201	pTrc99 A-*hifA*$_{Eag}$	St. Geme *et al*. (1996)
pJS201.1	pTrc99 A-*hifA*$_{Eag}$(Y215F)	This study
pJS201.2	pTrc99 A-*hifA*$_{Eag}$(Y215S)	This study
pJS201.3	pTrc99 A-*hifA*$_{Eag}$(Y215Stop)	This study
pJS201.4	pTrc99 A-*hifA*$_{Eag}$(G203 A)	This study
pJS201.5	pTrc99 A-*hifA*$_{Eag}$(G203S)	This study
pJS202	pMMB91-*hifB*$_{Eag}$	St. Geme *et al*. (1996)
pJS202.1	pMMB91-*hifB*$_{Eag}$(K119 A)	This study
pJS202.2	pMMB91-*hifB*$_{Eag}$(R9G)	This study
pJS204	pTrc99 A-*hifB*$_{Eag}$	This study
pJS205	pMMB91-*hifB*$_{F3031}$	This study
pJS206	pMMB91-*hifA*$_{Eag}$	This study
pJS206.1	pMMB91-*hifA*$_{Eag}$(Y215F)	This study
pJS206.2	pMMB91-*hifA*$_{Eag}$(Y215S)	This study
pJS206.3	pMMB91-*hifA*$_{Eag}$(Y215Stop)	This study
pJS206.4	pMMB91-*hifA*$_{Eag}$(G203 A)	This study
pJS206.5	pMMB91-*hifA*$_{Eag}$(G203S)	This study
pGK201	pMMB91-*hifA*$_{F3031}$	This study
pGK202	pTrc99 A-*hifB*$_{F3031}$	This study
pMF20	pOK12-*hifA*-*hifE*$_{F3031}$	This study
pGK203	pGEM5-*hifA*$_{PvuII}$-*hifE*$_{F3031}$	This study
pWW15	pGEM5-*hifA*-*hifE*$_{Eag}$	McCrea *et al*. (1994)
pWW15Δ*hifB*	pWW15 with in frame *hifB* deletion	This study
pWW1	pGEM5-*hifA*$_{BglII}$-*hifE*$_{Eag}$	Watson *et al*. (1994)

are identical except for the vector backbone and the inducible promoter. To construct pJS205, the *hifB*$_{F3031}$ gene was amplified from strain F3031 chromosomal DNA using the polymerase chain reaction (PCR) and then cloned into the polylinker site downstream of the *tac* promoter in pMMB91. To construct pGK201 and pGK202, the *hifA*$_{F3031}$ gene was liberated from pAW513 as an *Eco*RI–*Hin*dIII fragment and cloned into the polylinker downstream of either the *trc* promoter in pTrc99A or the *tac* promoter in pMMB91. For studies of the in vitro assembly of strain Eagan pili, pWW15 and pWW1 were employed. pWW15 contains the strain Eagan pilus gene cluster (*hifA*-*hifE*$_{Eag}$) cloned into the vector pGEM5, and pWW1 is a derivative of pWW15 truncated at the *hifA Bgl*II site (McCrea *et al*., 1994). For studies of the in vitro assembly of strain F3031 pili, pMF20 and pGK203 were used. pMF20 contains a 14 kb *Bgl*II fragment with the entire strain F3031 pilus gene cluster cloned into the *Bgl*II site of the vector pOK12. pGK203 contains the 5′ end of *hifA*$_{F3031}$ together with *hifB*-*hifE*$_{F3031}$ and was constructed by digesting pMF20 with *Pvu*II and *Bgl*II and then cloning the fragment into *Pvu*II–*Bgl*II-digested pGEM5.

Construction of hifA *and* hifB *point mutations and an in frame deletion of* hifB

Site-specific mutations in *hifB*$_{Eag}$ were generated using PCR and four different primers, including primers that correspond to the 5′ and 3′ ends of *hifB*$_{Eag}$ and a pair of complementary mutagenic primers that overlap the site of intended mutation. Initially, two separate reactions were performed using pJS201 as the template, including one with the 5′ primer and one mutagenic primer and the second with the 3′ primer and the complementary mutagenic primer. The resulting fragments were then combined as the template for a reaction performed with the 5′ and 3′ primers. *hifA*$_{Eag}$ mutations were generated more directly by introducing the mutation of interest into the *hifA*$_{Eag}$ 3′ primer and then amplifying the entire gene.

To create an in frame deletion in *hifB*$_{Eag}$ in the context of the rest of the *hif*$_{Eag}$ gene cluster, we modified the plasmid pWW15. Recombinant PCR was used to generate a *Bgl*II–*Eco*RI fragment, corresponding to the 5′ end of *hifA*$_{Eag}$, the *hifB*$_{Eag}$ gene with an internal 465-base pair deletion and the 5′ end of *hifC*$_{Eag}$. Subsequently, this fragment was inserted in place of the 2.94 kb *Bgl*II–*Eco*RI fragment in pWW15, generating pWW15Δ*hifB*.

Haemagglutination assays and pilus enrichment

E. coli transformants were incubated in Luria–Bertani broth at 37°C to an A600nm of 0.8, and gene expression (under control of the *tac* or *trc* promoter) was induced with 1 mM isopropylthio-β-d-galactoside (IPTG) for 1 h. To select for piliated organisms, enrichment was performed using a suspension of human erythrocytes, as has been previously described (Connor and Loeb, 1983). Criteria for pilus expression included a haemagglutination titre ≥1:8 (Pichichero *et al*., 1982), the presence of pili by negative staining transmission electron microscopy, reactivity on whole cell dot

immunoblots and inhibition of haemagglutination by pre-incubation with 100 μg ml^{-1} of GM1 (Sigma), a sialylated ganglioside that appears to mimic the pilus receptor structure (van Alphen *et al*., 1991).

Negative staining transmission electron microscopy

Suspensions of bacteria were collected from induced cultures and negative staining was performed with 0.5% uranyl acetate, as has beem previously described (St. Geme *et al*., 1991). Samples were examined using a Ziess 10A transmission electron microscope.

Cell fractionation and protein analysis

Periplasmic extracts were prepared as has been previously described (Slonim *et al*., 1992) and resolved on 12% polyacrylamide gels using SDS–PAGE. Samples were then electro-transferred to nitrocellulose membranes, which were blocked with 5% skim milk in Tris-buffered saline (TBS) and then probed with a rabbit polyclonal antiserum raised against either purified HifB obtained from strain Eagan or denatured HifA recovered from strain Eagan (St. Geme *et al*., 1996). Goat antirabbit IgG conjugated to alkaline phosphatase was employed as the secondary antibody, and reactivity was detected with nitroblue tetrazolium and 5-bromo-4-chloro-3-indolyl phosphate (Kirkegaard and Perry Laboratories).

In performing whole cell immunoblot assays, organisms were first fixed for 30 min with 4% paraformaldehyde in phosphate buffered saline (PBS). These organisms were subsequently washed three times with PBS, and suspensions were adjusted to an A_{600nm} of 0.6. Next, 100 μl volumes were applied to a nitrocellulose membrane resting on a single blotting sponge (VWR) in a Manifold I micro-sample filtration manifold apparatus (Schleicher and Schuell). After incubation for 30 min, low suction was applied to draw residual buffer through the manifold. The membrane was blocked in 5% skim milk in TBS for one hour, then probed with a rabbit polyclonal antiserum raised against the purified HifB–HifA complex from strain Eagan (St. Geme *et al*., 1996), an antiserum that is cross-reactive with strain F3031 pili. Goat antirabbit IgG conjugated to horseradish peroxidase (Sigma) was used as the secondary antibody and reactivity was detected using chemiluminescence with the SuperSignal enhanced substrate (Pierce) together with autoradiography film. As a control for membrane integrity, we performed simultaneous whole cell immunoblots with the anti-HifB antiserum, which should not react with whole cells as HifB is confined to the periplasm.

HifA modelling

Mutational analysis and sequence alignments indicated that HifA probably adopts a truncated Ig fold similar to that seen in the PapK structure. With this understanding, we used the PapK structure in the PapD–PapK complex (PDB accession code 1PDK) to model the structure of HifA. The PDB coordinates were not altered. Residues in PapK were colour coded according to sequence conservation, as described in the legend of Fig. 7, to reveal the likely locations of both conserved and variable regions in HifA.

Acknowledgements

This work was supported by Public Health Service grants 1RO1 DC-02873 and 1RO1 AI-44167 (J.W.S.). G.P.K. was supported by a fellowship from the Pediatric Infectious Diseases Society and by a Young Investigator's Matching Grant from the National Foundation for Infectious Diseases.

References

van Alphen, L., Poole, J., and Overbeeke, M. (1986) The Anton blood group antigen is the erythrocyte receptor for *Haemophilus influenzae*. *FEMS Microbiol Lett* **37**: 69–71.

van Alphen, L., Geelen-van den Broek, L., Blaas, L., van Ham, M., and Dankert, J. (1991) Blocking of fimbria-mediated adherence of *Haemophilus influenzae* by sialyl gangliosides. *Infect Immun* **59**: 4473–4477.

Amann, E., Ochs, B., and Abel, K.J. (1988) Tightly regulated *tac* promoter vectors useful for the expression of unfused and fused proteins in *Escherichia coli*. *Gene* **69**: 301–315.

Brinton, C.C. Jr, Carter, M.J., Derber, D.B., Kar, S., Kramarik, J.A., To, A.C., *et al*. (1989) Design and development of pilus vaccines for *Haemophilus influenzae* diseases. *Pediatr Infect Dis J* **8:** 554–561.

Bullitt, E., Jones, C.H., Striker, R., Soto, G., Jacob-Dubuisson, F., Pinkner, J.S., *et al*. (1996) Development of pilus organelle subassemblies in vitro depends on chaperone uncapping of a beta zipper. *Proc Natl Acad Sci USA* **93**: 12890–12895.

Carson, M. (1997) Ribbons. *Methods Enzymology* **277**: 493–505.

Choudhury, D., Thompson, A., Stojanoff, V., Langermann, S., Pinkner, J., Hultgren, S.J., and Knight, S.D. (1999) X-ray structure of the FimC-FimH chaperone-adhesin complex from uropathogenic *Escherichia coli*. *Science* **285**: 1061–1066.

Clemans, D.L., Marrs, C.F., Patel, M., Duncan, M., and Gilsdorf, J.R. (1998) Comparative Analysis of *Haemophilus influenzae hifA* (pilin) genes. *Infect Immun* **66**: 656–663.

Connor, E.M., and Loeb, M.R. (1983) A hemadsorption method for detection of colonies of *Haemophilus influenzae* type b expressing fimbriae. *J Infect Dis* **148**: 855–860.

Farley, M., Stephens, D.S., Kaplan, S.L., and Mason, Jr, E.O. (1990) Pilus- and non-pilus–mediated interactions of *Haemophilus influenzae* type b with human erythrocytes and human nasopharyngeal mucosa. *J Infect Dis* **161**: 274–280.

Forney, L.J., Marrs, C.F., Bektesh, S.L., and Gilsdorf, J.R. (1991) Comparison and analysis of the nucleotide sequences of pilin genes from *Haemophilus influenzae* type b strains Eagan and M43. *Infect Immun* **59**: 1991–1996.

Furste, J.P., Pansegrau, W., Frank, R., Bloker, H., Scholz, P., Bagdasarian, M., and Lanka, E. (1986) Molecular cloning of the plasmid RP4 primase region in a multi-host-range tacP expression vector. *Gene* **48**: 119–131.

Geluk, F., Eijk, P., van Ham, M., Jansen, H.M., and van Alphen, L. (1998) The fimbria gene cluster of nonencapsulated *Haemophilus influenzae*. *Infect Immun* **66**: 406–417.

Gilsdorf, J.R., McCrea, K.W., and Forney, L. (1990) Conserved and nonconserved epitopes among *Haemophilus influenzae* type b pili. *Infect Immun* **58**: 2252–2257.

Gilsdorf, J.R., Chang, H.Y., McCrea, K.W., and Bakaletz, L.O. (1992) Comparison of hemagglutinating pili of *Haemophilus influenzae* type b with similar structures of nontypeable *H. Influenzae*. *Infect Immun* **60**: 374–379.

Gilsdorf, J.R., Forney, L.J., and McCrea, K.W. (1993) Reactivity of antibodies against conserved regions of pilins of *Haemophilus influenzae* type b. *J Infect Dis* **167**: 962–965.

Gilsdorf, J.R., McCrea, K.W., and Marrs, C.F. (1997) Role of pili in *Haemophilus influenzae* adherence and colonization. *Infect Immun* **65**: 2997–3002.

van Ham, S.M., van Alphen, L., Mooi, F.R., and van Putten, J.P. (1994) The fimbrial gene cluster of *Haemophilus influenzae* type b. *Mol Microbiol* **13**: 673–684.

Holmgren, A., Kuehn, M.J., Branden, C.I., and Hultgren, S.J. (1992) Conserved immunoglobulin-like features in a family of periplasmic pilus chaperones in bacteria. *EMBO J* **11**: 1617–1622.

Hultgren, S.J., Jones, C.H., and Normark, S. (1996) Bacterial Adhesins and Their Assembly: In *Escherichia coli and Salmonella: Cellular and Molecular Biology*, 2nd edn. Neidhart, F.C., (ed.). Washington, DC: American Society for Microbiology Press, pp. 2730–2757.

Hung, D.L., Knight, S.D., Woods, R.M., Pinkner, J.S., and Hultgren, S.J. (1996) Molecular basis of two subfamilies of immunoglobulin-like chaperones. *EMBO J* **15**: 3792–3805.

Karlsson, K.A. (1989) Animal glycosphingolipids as membrane attachment sites for bacteria. *Annu Rev Biochem* **58**: 309–350.

Krasan, G.P., Cutter, D., Block, S.L., and St. Geme, III, J.W. (1999) Adhesin expression in matched nasopharyngeal and middle ear isolates of nontypeable *Haemophilus influenzae* from children with acute otitis media. *Infect Immun* **67**: 449–454.

Kuehn, M.J., Ogg, D.J., Kihlberg, J., Slonim, L., Flemmer, K., Bergfors, T., and Hultgren, S.J. (1993) Structural basis of pilus subunit recognition by the PapD chaperone. *Science* **262**: 1234–1241.

Loeb, M.R., Connor, E.M., and Penney, D. (1988) A comparison of the adherence of fimbriated and nonfimbriated *Haemophilus influenzae* type b to human adenoids in organ culture. *Infect Immun* **56**: 484–489.

McCrea, K.W., Watson, W.J., Gilsdorf, J.R., and Marrs, C.F. (1994) Identification of *hifD and hifE* in the pilus gene cluster of *Haemophilus influenzae* type b strain Eagan. *Infect Immun* **62**: 4922–4928.

McCrea, K.W., Watson, W.J., Gilsdorf, J.R., and Marrs, C.F. (1997) Identification of two minor subunits in the pilus of *Haemophilus influenzae*. *J Bacteriol* **179**: 4227–4231.

Mhlanga-Mutangadura, T., Morlin, G., Smith, A.L., Eisenstark, A., and Golomb, M. (1998) Evolution of the major pilus gene cluster of *Haemophilus influenzae*. *J Bacteriol* **180**: 4693–4703.

Orndorff, P.E., and Falkow, S. (1984) Organization and expression of genes responsible for type 1 piliation in *Escherichia coli*. *J Bacteriol* **159**: 736–744.

Palmer, K.L., and Munson, Jr, R.S. (1992) Construction of chimaeric genes for mapping a surface-exposed epitope on the pilus of non-typeable *Haemophilus influenzae*. *Mol Microbiol* **6**: 2583–2588.

Pichichero M.E., Loeb, M., Anderson, P., and Smith, D.H. (1982) Do pili play a role in pathogenicity of *Haemophilus influenzae* type b? *Lancet* **ii:** 960–962.

Rao, V.K., Krasan, G.P., Hendrixson, D.R., Dawid, S., and St. Geme, III, J.W. (1999) Molecular determinants of the pathogenesis of disease due to non-typable *Haemophilus influenzae*. *FEMS Microbiol Rev* **23**: 99–129.

Read, T.D., Dowdell, M., Satola, S.W., and Farley, M.M. (1996) Duplication of pilus gene complexes of *Haemophilus influenzae* biogroup aegyptius. *J Bacteriol* **178**: 6564–6570.

Read, R.C., Wilson, R., Rutman, A.A., Lund, V.J., Todd, H.C., Brain, A.P., *et al*. (1991) Interaction of nontypable *Haemophilus influenzae* with human respiratory mucosa *in vitro*. *J Infect Dis* **163**: 549–558.

St. Geme, III, J.W., Gilsdorf, J.R., and Falkow, S. (1991) Surface structures and adherence properties of diverse strains of *Haemophilus influenzae* biogroup aegyptius. *Infect Immun* **59**: 3366–3371.

St. Geme, III, J.W., Pinkner, J.S., Krasan, G.P., Heuser, J., Bullitt, E., Smith, A.L., and Hultgren, S.J. (1996) *Haemophilus influenzae* pili are composite structures assembled via the HifB chaperone. *Proc Natl Acad Sci USA* **93**: 11913–11918.

Sambrook, J., Fritsch, E.F., and Maniatis, T. (1989) *Molecular Cloning: a Laboratory Manual*, 2nd edn. Cold Spring Harbor, NY: Cold Spring Harbor Laboratory Press.

Sauer, F.G., Futterer, K., Pinkner, J.S., Dodson, K.W., Hultgren, S.J., and Waksman, G. (1999) Structural basis of chaperone function and pilus biogenesis. *Science* **285**: 1058–1061.

Slonim, L., Pinkner, J.S., Branden, C.I., and Hultgren, S.J. (1992) Interactive surface in the PapD chaperone cleft is conserved in pilus chaperone superfamily and essential in subunit recognition and assembly. *EMBO J* **11**: 4747–4756.

Soto, G.E., Dodson, K.W., Ogg, D., Liu, C., Heuser, J., Knight, S., et al. (1998) Periplasmic chaperone recognition motif of subunits mediates quaternary interactions in the pilus. *EMBO J* **17**: 6155–6167.

Stull, T.L., Mendelman, P.M., Haas, J.E., Schoenborn, M.A., Mack, K.D., and Smith, A.L. (1984) Characterization of *Haemophilus influenzae* type b pili. *Infect Immun* **46**: 787–796.

Thanassi, D.G., Saulino, E.T., and Hultgren, S.J. (1998) The chaperone/usher pathway: a major terminal branch of the general secretory pathway. *Curr Opin Microbiol* **1**: 223–231.

Turk, D.C. (1984) The pathogenicity of *Haemophilus influenzae*. *J Med Microbiol* **18**: 1–16.

Vieira, J., and Messing, J. (1991) New pUC-derived cloning vectors with different selectable markers and DNA replication origins. *Gene* **100**: 189–194.

Watson, W.J., Gilsdorf, J.R., Tucci, M.A., McCrea, K.W., Forney, L.J., and Marrs, C.F. (1994) Identification of a gene essential for piliation in *Haemophilus influenzae* type b with homology to the pilus assembly platform genes of gram-negative bacteria. *Infect Immun* **62**: 468–475.

Weber, A., Harris, R., Lohrke, S., Forney, L., and Smith, A.L. (1991) Inability to express fimbriae results in impaired ability of *Haemophilus influenzae* b to colonize the nasopharynx. *Infect Immun* **59**: 4724–4728.

Whitney, A.M., and Farley, M.M. (1993) Cloning and sequence analysis of the structural pilin gene of Brazilian purpuric fever-associated *Haemophilus influenzae* biogroup aegyptius. *Infect Immun* **61**: 1559–1562.

Yanisch-Perron, C., Vieira, J., and Messing, J. (1985) Improved M13 phage cloning vectors and host strains: nucleotide sequences of the M13mp 18 and pUC19 vectors. *Gene* **33**: 103–119.